Interference Modelling for Soft Frequency Reuse in Irregular Heterogeneous Cellular Networks

Conference Paper · July 2017

DOI: 10.1109/ICUFN.2017.7993813

Achonu Adejo
Newcastle University

Said Boussakta
Newcastle University

Jeffrey Neasham
Newcastle University

Interference Modelling for Soft Frequency Reuse in Irregular Heterogeneous Cellular Networks

Achonu Adejo*†, Said Boussakta* and Jeffrey Neasham*
*School of Electrical and Electronic Engineering, Newcastle University, United Kingdom
†Department of Telecommunications Engineering, Federal University of Technology Minna, Nigeria
†Email: a.o.adejo@newcastle.ac.uk, achonu.adejo@gmail.com

***Abstract*—Soft frequency reuse (SFR) has been proposed as a technique to address the problem of intercell interference (ICI) in cellular networks. A major challenge facing SFR implementation is the efficient allocation of scarce base station (BS) resources like bandwidth and power. This challenge further motivates the need for accurate network modelling, a requirement for optimal SFR algorithms. Particularly, the modelling and optimization of SFR in complex Heterogeneous cellular networks (HetNets) is a current problem in academia and the industry. In this paper, we present a new interference model for HetNets which considers the probabilistic nature of ICI in SFR. The interference probabilities from different BS tiers to the various user (UE) classes are computed. In combination with the analysis of macro BS transmit powers and distance relationships, new equations are also derived for UE signal-to-interference-ratio (SINR) and capacity. A detailed performance analysis is then presented for cases of both Hexagonal and Irregular macro BS placements. Our results show how macro and pico UE perform with respect to the BS power ratios, edge frequencies and placement of BS. This provides useful insights into the development of optimal SFR techniques for HetNets.**

***Index Terms*—Heterogeneous cellular network; inter-cell interference; Soft frequency reuse; Fractional frequency reuse; 4G/5G; resource allocation; irregular networks; self organised networks**

I. Introduction

Inter-cell interference (ICI) is a major challenge in current cellular communication systems employing Orthogonal Frequency Division Multiple Access (OFDMA). ICI severely limits the network capacity of these Long Term Evolution (LTE) and LTE-Advanced systems. The problem is aggravated by the demand for high data rates from intelligent mobile devices like smartphones and tablets. Consequently, the suppression of ICI is a key requirement in the design and optimization of modern cellular networks [1]. The degree of ICI experienced depends on factors like the amount of Frequency Reuse (FR) adopted and the layout of the network entities.

Soft Frequency Reuse (SFR) has been proposed in literature as an effective ICI coordination (ICIC) technique. It is one of the fractional-based FR schemes that requires the splitting of macro base station (BS) coverage regions. As opposed to the full FR scheme, SFR guarantees interference reduction especially for users/user equipment (UE) at the edge of the cells, termed edge UE. SFR is flexible and it provides a good balance between resource utilization and interference management in the network [2]. There is still need for the design of accurate network models describing SFR implementation in cellular networks. Furthermore, these networks are evolving via a new paradigm called Heterogeneous Cellular Networks (HetNets) as shown in Figs. 1 and 2. In HetNets, low powered BS e.g pico BS are used to overlay the traditional macro BS. This creates a multi-tier BS system that increases the network coverage and capacity, guaranteeing better UE performance [3]. Further gains can be derived when SFR concept is adopted in HetNets, but there is an added challenge of increased system complexity. In this paper, we present the analysis and simulation results for an improved SFR model that incorporates HetNets with irregular BS deployments. Compared to the traditional hexagonal macro BS models (Fig. 1), irregular deployment models (Fig. 2) are closer to the real cellular network deployments.

There are several approaches to the design and modelling of fractional-based FR cellular systems in literature. The problem of resource allocation is handled in two stages. In the first, frequency and other BS parameter assignment are performed for each BS. The second stage handles allocations to the individual UEs within a BS [2]. For this study, we are concerned with the analysis of models related to the first stage. In [4] and [5], the coverage area of irregular networks were divided into pixels and the data rates of the pixels were computed. However, only a single tier of macro BS deployment was considered in both cases. [6] and [7] used the methods of spatial point processes and stochastic geometry to develop analytical models, with [6] considering the case of HetNets. Valuable analytical expressions were provided which describe the average performance over the entire system. However, as pointed in [5], it is also helpful to evaluate the operational parameters over specific deployments using simulations. Coupled with the added benefit of analysing performance in or within regions of individual BS, the method of simulations is still beneficial for modelling.

For this study, we extend our work in [8], where only a single-tier model for FR schemes was considered and the transmit power to UEs was assumed constant in all BS regions. We provide a more detailed analysis of the SFR algorithm by exploiting the frequency overlaps between the BS bandwidth assignments. This affects the probability of interference from a particular BS to UEs in other BS within the same tier or in a different tier. This has an impact on the UE performance parameters like signal-to-interference ratio

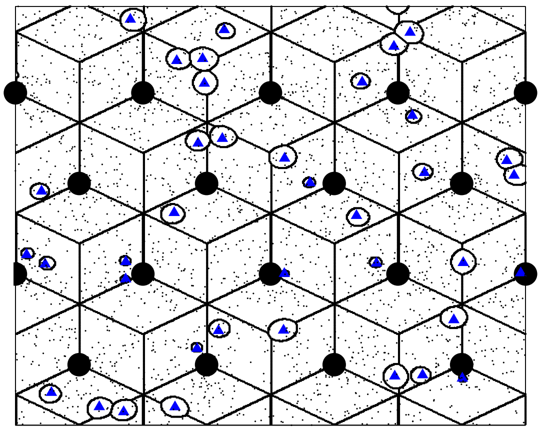

Fig. 1. Hexagonal HetNet with macro BS (big circles) and pico BS (triangles)

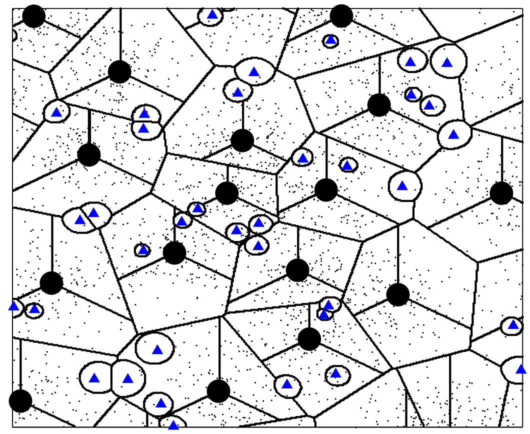

Fig. 2. Irregular HetNet with macro BS (big circles) and pico BS (triangles)

(SINR) and Capacity. Coupled with investigations into the distance relationships between UEs and BSs, and the effect of BS transmit power parameters, we formulate new analytical expressions for SINR and Capacity. Our results give deeper insights to the performance of HetNets and provide a useful framework for the design of optimal cellular systems.

The remaining part of this paper is organized thus: the system model is presented in Section II, Results are discussed in III and IV is for conclusion and future research.

II. System Model

A. Soft Frequency Reuse

In this section, we describe the basic SFR algorithm defining frequency assignment between BS in an irregular HetNet model. As shown in Fig. 3, macro BS utilize tri-sector antenna dividing their coverage regions into three sectors. The region of each sector is then divided into two; i.e the center and edge regions shown in the figure. Pico BS on the other hand utilize omnidirectional antenna and do not have sectors. Our analysis is restricted to the network performance within a reference macro BS sector, M. Other BS entities include I_m, the set of interfering macro BS sectors to M i.e $\{I_{m,1}, I_{m,2}\}$, I_p^C, the set of pico BS located within the center region of M and I_p^E, the set of pico BS located within the edge region of M.

Macro UE are classified into two based on their proximity to M, thus: 1) Edge UEs are located within the edge region of M, i.e close to the cell boundary. 2) Center UE locations are within the center region of M, closer to the sector antenna. Similar to the definition in [2], we use the concept of center of gravity (CoG) to describe UE positioning within a macro BS sector's region or Pico BS region. The CoG is the coordinate location of the mean position of all UE within any particular BS region. It is used to measure the average performance of UE within the region under consideration. The following UE entities are defined: U_m^C, the CoG for macro UE at the center of M, U_m^E, the CoG for macro UE at the edge of M, U_p^C, the CoG for pico UE connected to pico BS at the center region of M and U_p^E, the CoG for pico UE connected to pico BS at the edge region of M.

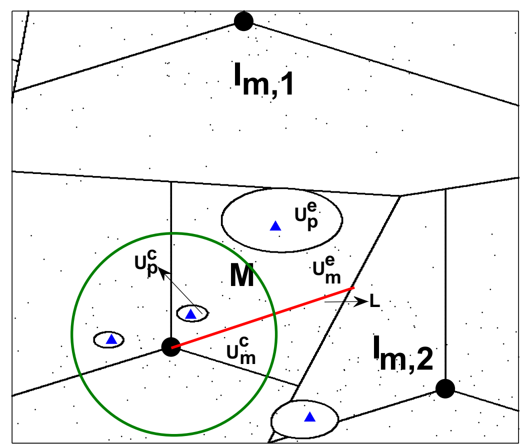

Fig. 3. System description

For SFR, the total system bandwidth is reused in all macro BS sector. However, as shown in Fig. 4, the frequency allocation in each sector is divided into two, for the center and edge regions. The edge regions of sector M receive a small allocation (E_M) but at a higher transmit power (P_e). The center UE within the center region of M are then assigned the remaining bandwidth (C_M) at lower power levels (P_c). Edge UE within neighbouring sectors, $I_{m,1}$, $I_{m,2}$ are assigned different frequencies ($E_{I,1}$, $E_{I,2}$) from E_M to reduce the effect of ICI. For pico UE connected to pico BS within both the center and edge of M, they are allocated only the same frequencies used by macro center UE in M, i.e ($F_{P,C}$, $F_{P,E}$), completely excluding any portion of E_M. Compared to [9] where pico UE also use similar frequencies to the macro edge UE, this model reduces the interference on Pico UE from the high edge transmissions.

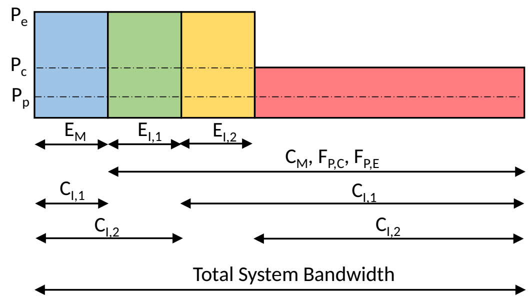

Fig. 4. Frequency/Power allocation for 3 neighbouring BS

B. Distance between system entities

We define $\{x, y\}$ as the Cartesian coordinate for M and r as its coverage radius. Imaginary line L in Fig. 3 is introduced to divide the coverage area of M into two and is used to define positional relationships between M and other BS and UE entities. Let γr be the distance between M and any interfering macro or pico BS, I. We also define ω as the angle formed between L and an imaginary line joining M to any I. Therefore the Cartesian coordinate for I is $\{(x + \gamma r \cos\omega), (y + \gamma r \sin\omega)\}$. Similarly, let the distance between M and the CoG for any macro or pico UE group within M be λr. Therefore the Cartesian coordinate of the CoG will be $\{(x + \lambda r \cos\theta), (y + \lambda r \sin\theta)\}$, where θ is the angle between L and the line joining M to the CoG.

An important parameter is the distance between the CoG and I which is derived in terms of their positional relationships with M as:

$$d = r\sqrt{\lambda^2 + \gamma^2 - 2\lambda\gamma(\cos(\omega - \theta))}. \quad (1)$$

C. Macro BS power parameter

Each macro BS sector has a power budget which determines how power is allocated to its center and edge transmissions [2]. Let μ be the ratio of the edge transmit power (P_e) to the center transmit power (P_c), i.e

$$\mu = \frac{P_e}{P_c}. \quad (2)$$

As Fig. 4 shows, in the SFR algorithm, $P_e > P_c$. In any sector e.g M, the total power budget P_t, is given by:

$$P_t = n_e P_e + n_c P_c, \quad (3)$$

where n_e and n_c are the number of edge and center UEs, respectively. Assuming the total number of UE is n_t, then

$$n_e + n_c = n_t, \quad (4)$$

and substituting into (3), for n_c from (4) and for P_c from (2), we obtain

$$P_e = \frac{\mu P_t}{n_e(\mu - 1) + n_t}. \quad (5)$$

Similarly,

$$P_c = \frac{P_t}{n_e(\mu - 1) + n_t}. \quad (6)$$

D. Interference analysis

Fig. 4 shows the SFR frequency and power allocation for the center and edge regions of sector M, two interfering macro BS and the center and edge pico BS within M. A key observation is the overlaps between the frequency allocations used for the different BS. As the intersections are partial for several cases, this gives rise to probabilities in the interference components which we define here. Let f_e be the size of the edge frequency allocation or edge physical resource block (PRB), i.e $f_e = E_M = E_{I,1} = E_{I,2}$. Also, let f_T be the total number of PRBs in the system. The following condition holds for our assumption that there are three subbands in the system:

$$2f_e \leq \frac{f_T - f_e}{2}. \quad (7)$$

1) Center macro UE interferences: The interferences are: β_1, the probability that a center macro UE (U_m^C) in M will receive interference from the edge transmission of neighbouring macro BS (I_m) using a similar PRB is given by:

$$\beta_1 = \frac{f_e}{f_T - f_e}. \quad (8)$$

β_2, the probability that U_m^C will use the same PRB as the center transmission of I_m and be interfered by it, is given by:

$$\beta_2 = \frac{f_T - 2f_e}{f_T - f_e}. \quad (9)$$

The probability that U_m^C will use the same PRB as any pico BS within the region (either center or edge) of M is 0.5.

2) Edge macro UE interferences: From the frequency allocation rule, edge macro UE in M are only interfered by center transmissions from I_m with a probability of 1.

3) Pico UE interferences: Based on (7), the rules for assigning center and edge Pico UE bandwidth are: $F_{P,C} = C_M$, $F_{P,E} = C_M/2$ and $F_{P,E} \cap (E_{I,1} + E_{I,2}) = 0$. The probability that any pico UE (connected to a pico BS within M) will be interfered by the center transmission or edge transmission of M is 1 or 0 respectively. The probability that a center pico UE (U_p^C) will be interfered by a pico BS (i.e I_p^C or I_p^E) within the center or edge region of M is 1 or 0 respectively. Similarly, the probability that an edge pico UE (U_p^E) will be interfered by I_p^C or I_p^E is 0 or 1 respectively.
β_3, the probability that U_p^C will be interfered by the center transmissions from neighbouring macro BS (I_m) is obtained based on (7) as:

$$\beta_3 = \frac{\frac{f_T - f_e}{2} - f_e}{\frac{f_T - f_e}{2}} = \frac{f_T - 3f_e}{f_T - f_e}. \quad (10)$$

The probability that an edge pico UE (U_p^E) will be interfered by the center transmissions from I_m is 1 due to (7).
β_4, the probability that U_p^C will be interfered by the edge transmissions from I_m is obtained also based on (7) as:

$$\beta_4 = \frac{f_e}{\frac{f_T - f_e}{2}} = \frac{2f_e}{f_T - f_e}. \quad (11)$$

$$SINR^i_{m,c} = \frac{P_{c,i}h(\lambda_c r)^{-\alpha}}{\sigma^2 + \sum\limits_{j=1, j\epsilon I_m}^{n^I_m} \beta_1 P_{e,j} h(d_{i,j})^{-\alpha} + \sum\limits_{j=1, j\epsilon I_m}^{n^I_m} \beta_2 P_{c,j} h(d_{i,j})^{-\alpha} + \sum\limits_{x=1, x\epsilon P_c}^{n^P_c} 0.5 P_{p,x} h(d_{i,x})^{-\alpha} + \sum\limits_{y=1, y\epsilon P_e}^{n^P_e} 0.5 P_{p,y} h(d_{i,y})^{-\alpha}}$$

$$= \frac{\frac{P_t}{n_{e,i}(\mu_i - 1) + n_{t,i}} h(\lambda_c r)^{-\alpha}}{\sigma^2 + \sum\limits_{j=1, j\epsilon I_m}^{n^I_m} \frac{(\mu_j f_e + f_T - 2f_e) P_t h[r\sqrt{\lambda_c^2 + \gamma_j^2 - 2\lambda_c \gamma_j (\cos(\omega_j - \theta_c))}]^{-\alpha}}{(n_{e,j}(\mu_j - 1) + n_{t,j})(f_T - f_e)} + \sum\limits_{x=1, x\epsilon P_c}^{n^P_c} \frac{P_{p,x} h[r\sqrt{\lambda_c^2 + \gamma_x^2 - 2\lambda_c \gamma_x (\cos(\omega_x - \theta_c))}]^{-\alpha}}{2} + \sum\limits_{y=1, y\epsilon P_e}^{n^P_e} \frac{P_{p,y} h[r\sqrt{\lambda_c^2 + \gamma_y^2 - 2\lambda_c \gamma_y (\cos(\omega_y - \theta_c))}]^{-\alpha}}{2}}. \tag{12}$$

$$SINR^i_{m,e} = \frac{P_{e,i}h(\lambda_e r)^{-\alpha}}{\sigma^2 + \sum\limits_{j=1, j\epsilon I_m}^{n^I_m} P_{c,j} h(d_{i,j})^{-\alpha}} = \frac{\frac{\mu_i P_t h(\lambda_e r)^{-\alpha}}{n_{e,i}(\mu_i - 1) + n_{t,i}}}{\sigma^2 + \sum\limits_{j=1, j\epsilon I_m}^{n^I_m} \frac{P_t h[r\sqrt{\lambda_e^2 + \gamma_j^2 - 2\lambda_e \gamma_j (\cos(\omega_j - \theta_e))}]^{-\alpha}}{n_{e,j}(\mu_j - 1) + n_{t,j}}}. \tag{13}$$

$$SINR^i_{p,c} = \frac{P_{p,i} h {d_{p,c}}^{-\alpha}}{\sigma^2 + P_{c,i} h(\lambda_{p,c} r)^{-\alpha} + \sum\limits_{k=1, k\epsilon I_m}^{n^I_m} \beta_3 P_{c,k} h(d_{i,k})^{-\alpha} + \sum\limits_{k=1, k\epsilon I_m}^{n^I_m} \beta_4 P_{e,k} h(d_{i,k})^{-\alpha} + \sum\limits_{j=1, j\epsilon P_c}^{n^P_c} P_{p,j} h(d_{i,j})^{-\alpha}}$$

$$= \frac{P_{p,i} h {d_{p,c}}^{-\alpha}}{\sigma^2 + \frac{P_t h(\lambda_{p,c} r)^{-\alpha}}{n_{e,i}(\mu_i - 1) + n_{t,i}} + \sum\limits_{k=1, k\epsilon I_m}^{n^I_m} \frac{(f_T - 3f_e + 2f_e \mu_k) P_t h[r\sqrt{\lambda_{p,c}^2 + \gamma_k^2 - 2\lambda_{p,c} \gamma_k (\cos(\omega_k - \theta_{p,c}))}]^{-\alpha}}{(n_{e,k}(\mu_k - 1) + n_{t,k})(f_T - f_e)} + \sum\limits_{j=1, j\epsilon P_c}^{n^P_c} P_{p,j} h[r\sqrt{\lambda_{p,c}^2 + \gamma_j^2 - 2\lambda_{p,c} \gamma_j (\cos(\omega_j - \theta_{p,c}))}]^{-\alpha}}. \tag{14}$$

$$SINR^i_{p,e} = \frac{P_{p,i} h {d_{p,e}}^{-\alpha}}{\sigma^2 + P_{c,i} h(\lambda_{p,e} r)^{-\alpha} + \sum\limits_{k=1, k\epsilon I_m}^{n^I_m} P_{c,k} h(d_{i,k})^{-\alpha} + \sum\limits_{j=1, j\epsilon P_e}^{n^P_e} P_{p,j} h(d_{i,j})^{-\alpha}}$$

$$= \frac{P_{p,i} h {d_{p,e}}^{-\alpha}}{\sigma^2 + \frac{P_t h(\lambda_{p,e} r)^{-\alpha}}{n_{e,i}(\mu_i - 1) + n_{t,i}} + \sum\limits_{k=1, k\epsilon I_m}^{n^I_m} \frac{P_t h[r\sqrt{\lambda_{p,e}^2 + \gamma_k^2 - 2\lambda_{p,e} \gamma_k (\cos(\omega_k - \theta_{p,e}))}]^{-\alpha}}{(n_{e,k}(\mu_k - 1) + n_{t,k})} + \sum\limits_{j=1, j\epsilon P_e}^{n^P_e} P_{p,j} h[r\sqrt{\lambda_{p,e}^2 + \gamma_j^2 - 2\lambda_{p,e} \gamma_j (\cos(\omega_j - \theta_{p,e}))}]^{-\alpha}}. \tag{15}$$

E. Signal-to-interference-noise-ratio (SINR) equations

The SINR of the ith macro center UE, $U^C_{m,i}$ connected to sector M is given in (12) where n^I_m,, n^P_c, n^P_e are the number of interfering macro BS in the set I_m, the number of interfering pico BS within the center region of M, in the set I^C_p and the number of interfering pico BS within the edge region of M, in the set I^E_p, respectively. h, σ^2, α represent the fading component, noise component and the path loss exponent respectively. $P_{a,b}$ is the transmit power from a BS represented by a to the bth UE being analysed and $d_{b,a}$ is defined as the distance between the bth UE and the BS represented by a. Similarly, the SINR of the ith macro edge user, $U^E_{m,i}$ connected to M is given in (13), the SINR of the ith pico UE, U^C_p within the center region of M is stated in (14) and the SINR of the ith pico UE, U^E_p within the edge region of M is given by (15).

F. Capacity equations

The Capacity for the ith macro center UE is given by:

$$Cap^i_{m,c} = min[\mathcal{B}_m, \frac{(f_T - f_e)\mathcal{B}_s}{n_{t,i} - n_{e,i}}][\log_2(1 + SINR^i_{m,c})], \tag{16}$$

where $\mathcal{B}_m$ is the maximum bandwidth that can be offered a UE and $\mathcal{B}_s$ is the bandwidth per PRB.

Similarly for the ith macro edge UE, the Capacity is:

$$Cap^i_{m,e} = min[\mathcal{B}_m, (\frac{f_e \mathcal{B}_s}{n_{e,i}})][\log_2(1 + SINR^i_{m,e})], \tag{17}$$

For the ith pico center UE, the Capacity is:

$$Cap^i_{p,c} = min[\mathcal{B}_m, \frac{(f_T - f_e)\mathcal{B}_s}{2n_{p,c}}][\log_2(1+SINR^i_{p,c})], \tag{18}$$

Lastly, the Capacity of the ith typical pico edge UE is:

$$Cap^i_{p,e} = min[\mathcal{B}_m, \frac{(f_T - f_e)\mathcal{B}_s}{2n_{p,e}}][\log_2(1+SINR^i_{p,e})], \tag{19}$$

where $n_{p,c}$ and $n_{p,e}$ represent the total number of center and edge UE connected to a pico BS under consideration.

III. Results and Analysis

In this section, we present the analysis for Hexagonal (uniform) and Irregular (random) macro HetNets using the model proposed in section II. We investigate the effect of various BS parameter on the performance of the different groups of macro and pico UE. The results are presented for UE within a reference macro BS region, subject to external macro interferences.

A. Simulation Parameters

We assume two interfering macro BS to the UE within the reference macro BS, one pico BS in its center region and two pico BS in its edge region. Each macro BS has the following parameters, $P_t = 43$dBm, $r = 0.5$Km and for the pico BS, $P_p = 4/48$dBm. In addition, we assume the following, total PRB $= 48$ and assuming fully connected and active BS regions, we have 1 PRB per UE ($n_t = n_p = 48$). n_e, n_t, f_e and f_T are assumed to be the same for all macro BS with $n_e = 9$. For the macro UE distance parameters,

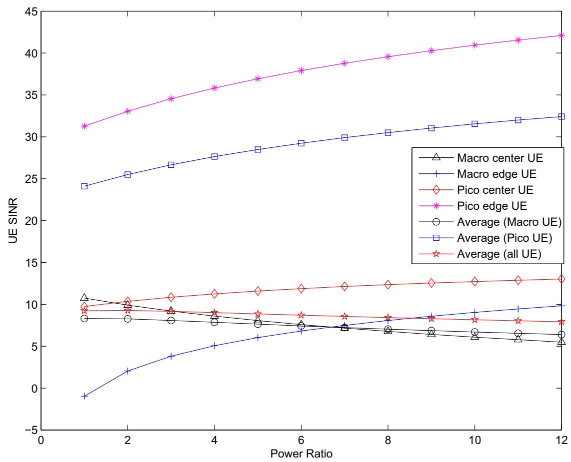

Fig. 5. UE SINR for different power ratios

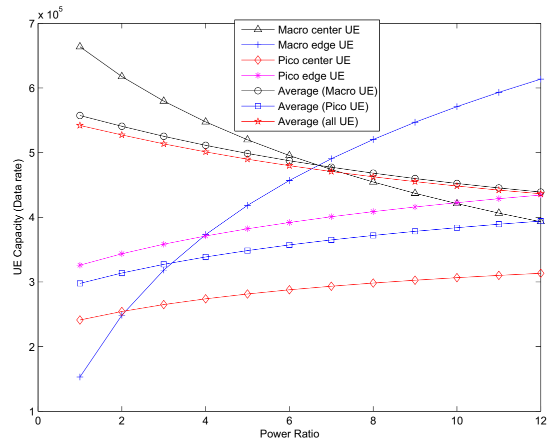

Fig. 6. UE Capacity for different power ratios

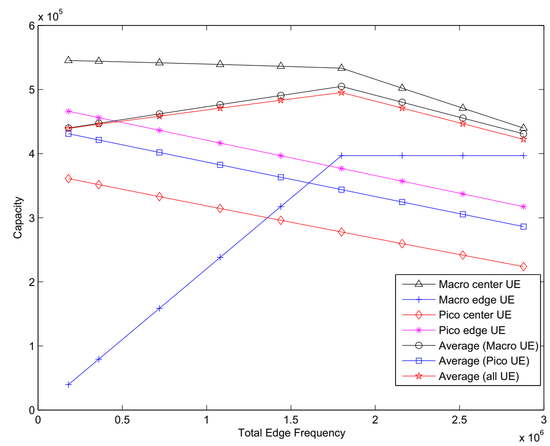

Fig. 7. UE Capacity for different edge frequencies

$\lambda_c = 0.25, \lambda_e = 0.9, \theta_c = \theta_e = 0^o$. For the pico BS, $\gamma_{p,c} = 0.4, \gamma_{p,e} = [0.75, 0.75], \omega_{p,c} = 30^o, \omega_{p,e} = [-30^o, 30^o]$. For the pico UE distance parameters, $d_{p,c} = d_{p,e} = (0.9 * P_p)/P_t, \lambda_{p,c} = \gamma_{p,c} + d_{p,c}, \lambda_{p,e} = \gamma_{p,e} + d_{p,e}$. Other parameter assignments include $h = 1, \alpha = 3$ and $\sigma = 0$. The system bandwidth considered is 10MHz and bandwidth per PRB, $\mathcal{B}_s = \mathcal{B}_m = 180$KHz. Simulations were made for the HetNet using MATLAB. We compute the SINR and Capacity for the CoG for macro edge and center UE, and pico UE (both in the center and edge regions). We also compute the average values for macro UE, pico UE and all UE.

B. Hexagonal macro BS

The proposed HetNet model is deployed in a Hexagonal network as depicted in Fig. 1. The following additional parameters were adopted: $\gamma_{m,1} = \gamma_{m,2} = \sqrt{3}, \omega_m = [-30^o, 30^o]$. Figs. 5 and 6 show respectively the SINR and Capacity curves for the hexagonal HetNet when the macro power ratio, μ is varied. We assume that μ is the same in all macro BS and $f_e = n_e \mathcal{B}_s$. The SINR performance for pico edge UE is the best for all cases of μ, with a value of about 220% over the pico center UE in most cases. It also outperforms the macro center and edge UE by even higher amounts. This is because, as (15) and Fig. 4 show, we have adopted an SFR HetNet variant that shields pico edge UE from macro BS edge interferences. As expected from (12) and (13), the macro edge UE SINR varies directly with μ, while that of macro center varies indirectly. The unique performance of each class of UE shows that it is preferable to analyse them separately rather than computing the averages for all UE in the system.

Fig. 6 shows the macro UEs outperforming the pico UEs in terms of Capacity. This is partly due to our assumption of the worst case scenario (fully connected UE with $n_t = n_p = 48$) in all BS regions. (18) and (19) show that a reduction in $n_{p,c}$ or $n_{p,e}$ would result in an increase in the Capacity results. The results show that even though pico UE generally have the higher SINR (for the SFR variant we have adopted), the same is not always true for the Capacity. The number of UE connected to a pico UE is a significant parameter affecting performance. It will be interesting to adopt different SFR variants and study the impact on SINR and Capacity of pico UE. We also observe that there is a meeting point between macro center and edge UE in the Capacity curve. This justifies the need for the development of optimization frameworks that optimize μ based on defined criteria. Even though macro edge UE have been defined as more vulnerable than macro center UE to ICI, very high values of μ can result in lower SINR and Capacity performances for macro center UE. An optimization scheme with a goal to maximize macro edge UE performance would have to be balanced by setting acceptable performance limits for the macro center and pico UE. Subsequently, we will restrict our results and analysis presented to just UE Capacity curves as these indicate UE data rates.

In Fig. 7, the effect on Capacity performance is analysed when f_e is varied when $\mu = 4.5$. The Capacity for macro edge UE increases with f_e to a maximum, while for the macro center UE, it initially remains constant and falls off later. The pico UE Capacities reduce with increasing f_e. These results are consistent with (16) - (19), where a maximum UE

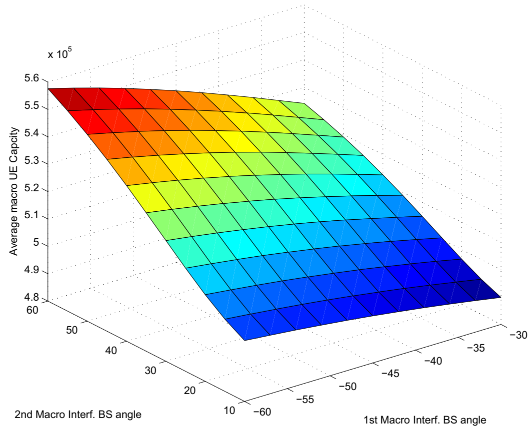

Fig. 8. Average macro UE Capacity for different macro BS combinations

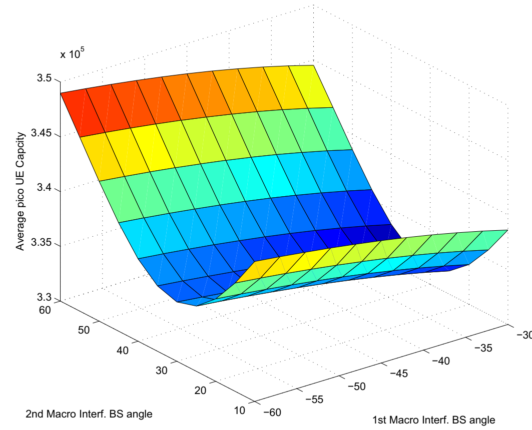

Fig. 9. Average Pico UE Capacity for different macro BS combinations

frequency allocation ($\mathcal{B}_m$) is specified for fairness. Again, we observe that an optimal scheme should take all UE groups into consideration considering their peculiar relationships with the BS parameters.

C. Irregular BS

We extend our SFR model to the case of Irregular macro BS HetNets where the macro BS deployments are not uniform. Assuming $\mu = 4.5, n_e = 9, \gamma_m = [\sqrt(3), \sqrt(3)]$, we set different values of $\omega_{m,1}$ and $\omega_{m,2}$. $\omega_{m,1}$ varies between -60^o to -30^o while $\omega_{m,2}$ between 10^o to 60^o and the $3D$ plots in Figs. 8 and 9 show the different average Capacities for macro and pico UE respectively. The figures show that the average Capacities are highest when the interfering macro BS are at the farthest distance ($\omega_{m,1} = -60$ and $\omega_{m,2} = 60$) from the CoG of the UE. Similarly, the least values for Capacities occur when the interfering macro BS are closest to the UE. However, this occurs at different combinations of $\omega_{m,1}$ and $\omega_{m,2}$ because of the different locations of the CoG for macro and pico UE. This further justifies the need for a carefully designed optimal SFR technique.

IV. Conclusion

In this paper, we have proposed a new model for the analysis of ICI in HetNets employing the SFR algorithm. The method takes into consideration how SFR introduces peculiar interferences probabilities for different classes of UE within the system. We derived equations that show how SINR and Capacity for different UE depend on the interferences from both macro and pico UE. The proposed model also addressed the case of irregular macro BS placements through consideration of the distance relationships between network entities. In addition, BS transmit power equations were used to account for power budgeting. Performance analysis was presented for the cases of hexagonal and irregular macro BS. Results show notable differences in the performance of macro and pico UE and even within each broad class of UE. SINR and Capacity performance showed some variations which confirms the transmit power, edge frequency allocation and number of edge UE are parameters that affect performance in different ways. This emphasizes the need for the development of optimal SFR schemes that consider the different BS parameters and their effect on the different UE classes. This motivates our current research work where we exploit distributed optimization over multilevel SFR HetNet systems.

Acknowledgment

Achonu Adejo wishes to thank the National IT Development Agency, NITDA in Nigeria for supporting this research.

References

[1] A. S. Hamza, S. S. Khalifa, H. S. Hamza, and K. Elsayed, "A survey on inter-cell interference coordination techniques in ofdma-based cellular networks," *IEEE Communications Surveys Tutorials*, vol. 15, no. 4, pp. 1642–1670, Fourth 2013.

[2] O. G. Aliu, M. Mehta, M. A. Imran, A. Karandikar, and B. Evans, "A new cellular-automata-based fractional frequency reuse scheme," *IEEE Transactions on Vehicular Technology*, vol. 64, no. 4, pp. 1535–1547, April 2015.

[3] A. Khandekar, N. Bhushan, J. Tingfang, and V. Vanghi, "Lte-advanced: Heterogeneous networks," in *2010 European Wireless Conference (EW)*, April 2010, pp. 978–982.

[4] L. Chen and D. Yuan, "Soft frequency reuse in large networks with irregular cell pattern: How much gain to expect?" in *2009 IEEE 20th International Symposium on Personal, Indoor and Mobile Radio Communications*, Sept 2009, pp. 1467–1471.

[5] D. G. G, M. Garcia-Lozano, S. R. Boque, and D. S. Lee, "Optimization of soft frequency reuse for irregular lte macrocellular networks," *IEEE Transactions on Wireless Communications*, vol. 12, no. 5, pp. 2410–2423, May 2013.

[6] T. D. Novlan, R. K. Ganti, A. Ghosh, and J. G. Andrews, "Analytical evaluation of fractional frequency reuse for heterogeneous cellular networks," *IEEE Transactions on Communications*, vol. 60, no. 7, pp. 2029–2039, July 2012.

[7] T. D. Novlan, H. S. Dhillon, and J. G. Andrews, "Analytical modeling of uplink cellular networks," *IEEE Transactions on Wireless Communications*, vol. 12, no. 6, pp. 2669–2679, June 2013.

[8] A. Adejo and S. Boussakta, "Performance analysis of frequency reuse techniques under varying cellular network scenarios," in *2016 IEEE Wireless Communications and Networking Conference*, April 2016, pp. 1–6.

[9] N. Saquib, E. Hossain, and D. I. Kim, "Fractional frequency reuse for interference management in lte-advanced hetnets," *IEEE Wireless Communications*, vol. 20, no. 2, pp. 113–122, April 2013.